

New clues on outburst mechanisms and improved spectroscopic elements of the black-hole binary V4641 Sagittarii ^{*}

C. Lindström¹, J. Griffin¹, L. L. Kiss^{1,†,‡}, M. Uemura^{2,3}, A. Derekas^{1,4}, Sz. Mészáros⁵, P. Székely⁶

¹*School of Physics A28, University of Sydney, NSW 2006, Australia*

²*Departamento de Física, Facultad de Ciencias Físicas y Matemáticas, Universidad de Concepción, Casilla 160-C, Concepción, Chile*

³*Yukawa Institute for Theoretical Physics, Kyoto University, Kyoto 606-8502, Japan*

⁴*School of Physics, Department of Astrophysics and Optics, University of New South Wales, NSW 2052, Australia*

⁵*Department of Optics and Quantumelectronics, University of Szeged, Hungary*

⁶*Department of Experimental Physics and Astronomical Observatory, University of Szeged, Hungary*

Accepted ... Received ...; in original form ..

ABSTRACT

We present spectroscopic observations of the black-hole binary V4641 Sagittarii, obtained between 4th July 2004 and 28th March 2005, which cover the minor outburst of the star in early July 2004 and quiescence variations on 19 nights scattered over six months. During the outburst, the star peaked approximately 3 magnitudes brighter than usual, and our spectra were dominated by broad hydrogen, helium and iron emission lines. The very first spectra showed P Cygni profiles, which disappeared within a few hours, indicating rapid changes in matter ejection. The $H\alpha$ line had multiple components, one being a broad blue-shifted wing exceeding 5000 km/s. During a simultaneously observed 10-min photometric flare-up, the equivalent width of the $H\alpha$ line temporarily decreased, implying that it was a flare of the continuum. The overall spectral appearance was similar to that observed in the 1999 September active phase, which suggests that similar mass-ejection processes were associated with both eruptions. In quiescence, the spectra were those of the early-type secondary star showing its orbital motion around the primary. By measuring cross-correlation radial velocities, we give an improved set of spectroscopic elements. Whereas we measure the same velocity amplitude ($K_2 = 211.3 \pm 1.0 \text{ km s}^{-1}$), within errors, as Orosz et al. (2001), our centre-of-mass velocity ($\gamma = 72.7 \pm 3.3 \text{ km s}^{-1}$) differs significantly from the previously published value ($107.4 \pm 2.9 \text{ km s}^{-1}$). However, we find evidence that the difference is caused by a systematic error in data reduction in the previous study, rather than by gravitational effects of an invisible third component.

Key words: X-rays: binaries – black hole physics – stars: individual: V4641 Sgr

1 INTRODUCTION

The X-ray transient V4641 Sgr (SAX J1819.3–2525) is a unique black-hole binary, which has attracted considerable interest since its major outburst in September 1999, where it peaked at $V \sim 8.8$ (Stubbings 1999). Even in quiescence, the star is fairly bright at $V \approx 13.7$ mag. It has an orbital period of 2.817 days, and is located at a distance of $\sim 7 - 12$ kpc toward the galactic bulge (Orosz et al. 2001). The total mass of the system lies between $14 - 20 M_{\odot}$ with a

black hole primary of $\sim 9 - 12 M_{\odot}$ (Orosz et al. 2001). Given its moderate inclination ($60 - 70^{\circ}$, Orosz et al. 2001), the system does not show eclipses and the quiescence light curve is dominated by ellipsoidal variability. The secondary was classified as a B9III star, being one of the most luminous secondary stars known in dynamically established black-hole binaries (Orosz et al. 2001). The large eruption in 1999 was associated with superluminal jet ejection and was followed by a series of smaller outbursts in the last few years. These involved violent flashes and rapid variability, making this relatively bright system a key target for understanding the processes associated with black hole binaries.

The activity of V4641 Sgr has been variable since the 1999 September outburst. As a faint X-ray source it was discovered independently by RXTE (Markwardt et al. 1999) and BeppoSax (in't

^{*} Based on data obtained at the Mount Stromlo and Siding Spring Observatories

[†] On leave from University of Szeged, Hungary

[‡] E-mail: l.kiss@physics.usyd.edu.au

Zand et al. 1999) in 1999 February. The 1999 September event, peaking at 12.2 Crab in the 2–12 keV band, was extremely rapid in its rise and decay across radio, optical and X-ray wavelengths. In X-rays, a brief but dramatic eruption occurred on Sept. 15–16, 1999, showing remarkably rapid fluctuations (Wijnands & van der Klis 2000). The optical decay lasted about two days (e.g. Chaty et al. 2003), while the radio transient was detected for a further three weeks. The measurable proper motion of the resolved radio structures indicated superluminal jet ejection (Hjellming et al. 2000). Subsequent quiescence observations led Orosz et al. (2001) to measuring the most accurate system parameters so far, which revealed the massive stellar black hole primary and the nature of the early-type secondary star.

The second major outburst occurred in 2002 May, when unprecedented rapid optical fluctuations were detected (Uemura et al. 2002). The short time-scale of the large-amplitude variations indicated that the inner region of the accretion disk made a significant contribution to the optical flux, implying strong non-thermal emission in the optical (Uemura et al. 2002, 2004b). Another outburst in 2003 August was very similar to the one in the previous year, leading Uemura et al. (2004a) to the conclusion that the two eruptions had the same nature. They also suggested the possibility of recurrent outbursts on a time-scale of 1–2 years.

This estimate of the time-scale was supported by R.Stubbings’s visual report of a fourth major outburst on 2004 July 4.368 UT, where the star peaked at around $V \approx 11.1$ mag (Uemura et al. 2005). Coincidentally, the star was detected with the RXTE at 8.2 mCrab flux (2–10 keV) on July 3.496, roughly eight times fainter than during the outburst in 2003 (Swank 2004) and three orders of magnitude dimmer than in the large 1999 September event. VLA observations clearly detected the outburst in radio, as a 12.5 mJy source at 1.425 GHz, with a steep spectrum (Rupen et al. 2004). A day later, V4641 Sgr was already close to its quiescence level (Revnivtsev et al. 2004), although very rapid, post-outburst flares of 1 mag were seen as late as 17 days after the main outburst (Bikmaev et al. 2004, Uemura et al. 2005). Most recently, a new active phase occurred in late June, 2005, when V4641 Sgr was detected in a very similar outburst like those in 2002, 2003 and 2004 (Swank et al. 2005, Khamitov et al. 2005, Buxton et al. 2005).

We started spectroscopic monitoring of the system on 2004 July 4.48, roughly two hours after the 2004 outburst was reported via electronic mailing lists, with a few optical and near-infrared spectra (an early report was given by Kiss & Mészáros 2004). In all follow-up observations between 2004 September and 2005 March were taken in the quiescence of V4641 Sgr and they allowed us to measure an improved set of spectroscopic elements.

Some of the important questions we wish to address in this paper are as follows. What is the driving mechanism behind these recurrent outbursts? What sort of processes accompany an eruption? How much are the 2002–2004 outbursts different from the major one in 1999 September? Which system parameters can be better constrained using our dataset? We describe the observations in Sect. 2; Sect. 3 discusses the outburst spectra, while quiescence data are presented in Sect. 4. Discussion of the above questions can be found in Sect. 5 and the paper concludes in Sect. 6.

2 OBSERVATIONS AND DATA REDUCTIONS

The observations were carried out with the 2.3m telescope at the Siding Spring Observatory, Australia. Four sets of observations

were obtained: 2004 July 4, during the outburst; four nights in late 2004 September, nine nights in 2004 October/November and six nights in 2005 March, all in quiescence (see Table 1 for details). All spectra were taken with the Double Beam Spectrograph using 1200 mm^{-1} gratings in both arms (except in 2005 March, when a CCD failure prevented the use of the blue arm). The exposure time ranged between 240–900 s for the outburst spectra and was 1200 s in quiescence. The dispersion was 0.55 \AA px^{-1} , leading to a nominal resolution of about 1 \AA . In addition to the V4641 Sgr spectra, we regularly observed a telluric standard (HD 177724) and several radial velocity standard stars (HD 187691, β Vir, HR 3383). The latter were used to measure cross-correlation radial velocities in quiescence.

All spectra were reduced with standard tasks in IRAF¹. Reduction consisted of bias and flat field corrections, aperture extraction, wavelength calibration and continuum normalization. We did not attempt flux calibration because the conditions were generally non-photometric. We checked the consistency of wavelength calibrations via the constant positions of strong telluric features, which proved the stability of the system. Radial velocities were determined with the task *fxcor*, including barycentric corrections. Different velocity standards have shown that our absolute velocity frame was stable to within $\pm 2\text{--}3 \text{ km s}^{-1}$.

3 SPECTRA OF THE 2004 JULY OUTBURST

About two hours after the first visual report arrived, we took three spectra in both the blue and red arms (between July 4.48–4.50 UT). The latter was observing in the near-infrared, showing spectra dominated by the Paschen series. Five hours later, we went back to the star to take another near-infrared spectrum, after which we switched to the $H\alpha$ region. Thereafter we took spectra in both arms continuously until the object was too low over the horizon. We obtained a total of 24 spectra, which showed remarkable changes with time. Orbital phases were assigned using the following ephemeris for the shallower minimum of the ellipsoidal variability (Uemura et al., in preparation; see also Sect. 4 for the spectroscopic ephemeris):

$$\text{HJD}_{\text{min}} = 2453154.67359 + 2.81728 \times E \quad (1)$$

Using this ephemeris, the orbital phases covered by our data ranged between 0.89 and 0.99, where 1.00 corresponds to the secondary passing in front of the black hole.

We show a representative collection of the three spectral regions observed during outburst in Figs 1–2 and Fig. 5. Lines of hydrogen and helium dominate the spectrum with weaker detections of Fe II, Mg II and Si II. Rapid variations in line profiles between spectra indicate a high and unpredictable activity, whereas a large range of gas velocities is reflected in the broad emission profiles.

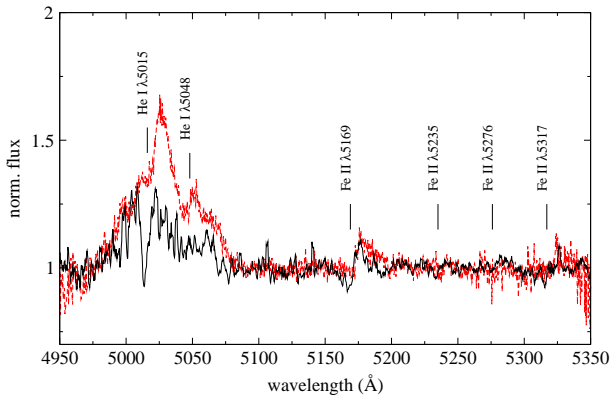
3.1 Blue region

Here we identify the strong blend of the He I $\lambda 5015$ and $\lambda 5048$ lines and four Fe II lines, of which the Fe II $\lambda 5169$ is the strongest (Fig. 1), while Fe II $\lambda 5235$ and Fe II $\lambda 5276$ are marginally detected. Line profiles of He I $\lambda 5015$ exhibited a rapid change between the

¹ IRAF is distributed by the National Optical Astronomy Observatories, which are operated by the Association of Universities for Research in Astronomy, Inc., under cooperative agreement with the National Science Foundation.

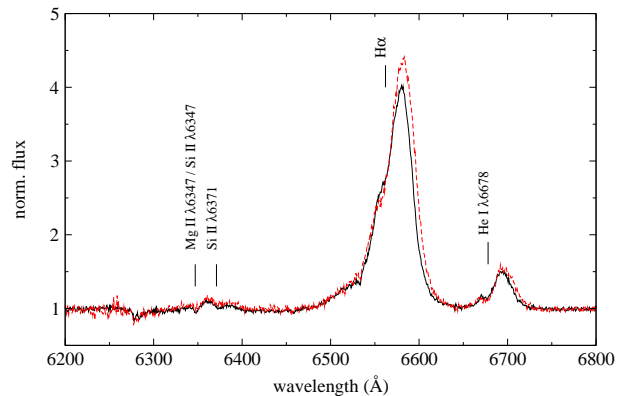
Table 1. Observation log. ‘HJD’ refer to the range in heliocentric Julian Dates, marked by the first and the last spectrum on any given night.

Date	HJD (2,453,000+)	Red arm		Blue arm	
		Wavelength range (Å)	No. of spectra	Wavelength range (Å)	No. of spectra
<i>Outburst</i>					
2004 July 4	190.9870–191.2176	8043–8972	4		
	191.2271–191.2652	6047–7005	10		
	190.9870–191.2629			4940–5383	10
<i>Quiescence</i>					
2004 Sept 25	274.013–274.066	5786–6748	4	4510–4973	4
2004 Sept 26	274.882–275.038	5786–6748	8	4510–4973	8
2004 Sept 27	275.878–276.027	5786–6748	2	4510–4973	2
2004 Sept 28	276.878–277.026	5786–6748	7	4510–4973	7
2004 Oct 25	303.894	5794–6756	1	4785–5233	1
2004 Oct 26	304.917–304.932	5794–6756	2	4785–5233	2
2004 Oct 27	305.899–305.916	5794–6756	2	4785–5233	2
2004 Oct 28	306.894–306.908	5794–6756	2	4785–5233	2
2004 Oct 29	307.889–307.903	5794–6756	2	4785–5233	2
2004 Oct 30	308.913–308.927	5794–6756	2	4785–5233	2
2004 Oct 31	309.905	5794–6756	1	4785–5233	1
2004 Nov 1	310.899	5794–6756	1	4785–5233	1
2004 Nov 2	311.915	5794–6756	1	4785–5233	1
2005 Mar 21	451.232–451.247	5794–6756	2		
2005 Mar 24	454.245–454.260	5794–6756	2		
2005 Mar 25	455.272–455.287	5794–6756	2		
2005 Mar 26	456.260–456.275	5794–6756	2		
2005 Mar 27	457.195	5794–6756	1		
2005 Mar 28	458.199–458.213	5794–6756	2		


Figure 1. The blue region at July 4.481 UT (black/solid line) and 6.4 hours later at July 4.748 UT (red/dashed line).

early and the late phase, separated by more than five hours. During the early phase, it contained a red-shifted peak, a deep absorption and a blue-shifted peak. The blue peak apparently has a narrow peak with a broad shoulder. During the late phase, the line profile becomes a complex emission line with a strong red peak, a blue component and a broad blue wing. The full width at zero intensity (FWZI) reached about 5000 km s^{-1} , although it is difficult to measure due to the close blend.

Of the four Fe II lines, the strongest Fe II $\lambda 5169$ line showed a clear P Cyg-like profile in the early phase and possibly in the late phase. Similar features are also visible in the Fe II $\lambda 5317$ line. The absorption components were blue-shifted by $500\text{--}600 \text{ km s}^{-1}$, relative to the emission peak.


Figure 2. The $H\alpha$ region at July 4.727 UT (black/solid line) and July 4.765 UT (red/dashed line).

3.2 $H\alpha$ region

This region was dominated by a very broad and strong $H\alpha$ line, the He I $\lambda 6678$ line and weak Mg II/Si II emission features. The FWZI of the $H\alpha$ line exceeded 5000 km s^{-1} , with an equivalent width (EW) of about $130\text{--}140 \text{ \AA}$. The asymmetric line profile of the $H\alpha$ line can be explained by the presence of a few (at least three) distinct components, namely a strong red-shifted component, a weaker blue-shifted component and a broad wing. The He line had approximately the same structure. Both profiles suggest the presence of a high-velocity outflow component, which is strikingly similar to what was reported in the 1999 September outburst (Orosz et al. 2001, Chaty et al. 2003).

The roughly one hour of continuous observations in the $H\alpha$ region revealed further interesting features. Firstly, there was a sig-

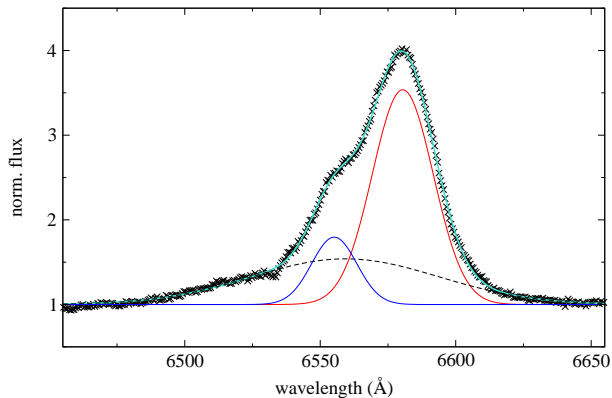


Figure 3. Three-component Gaussian fit to the H α line.

nificant change in the line profile over the one hour interval. Secondly, from Fig. 2, it is apparent that the red peak moved further redward, while the blue component moved significantly blueward. The width of the red component also increased with time, while very similar changes occurred in the He I $\lambda 6678$ line. To quantify these changes, we fitted multiple Gaussian components to all 10 H α profiles. A sample fit is shown in Fig. 3. It turned out that the red peak moved by $\sim 80 \text{ km s}^{-1}$ towards red, while the blue peak moved almost twice as much, $\sim 150 \text{ km s}^{-1}$ towards blue. Their widths also changed from spectrum to spectrum, indicating significant changes in line profiles.

In parallel with these H α spectra, one of us (M.U.) made simultaneous CCD photometric observations in Chile, using a 30 cm telescope at Universidad de Concepcion. These observations covered a 10-minute flare with 0.2 mag amplitude at JD=2,453,191.233, which just coincided with taking two spectra in Australia. The one-hour interval of simultaneous photometry and spectroscopy allowed us to investigate unprecedented detail into the rapid variability of the system (the full photometric behaviour of the 2004 eruption is discussed in Uemura et al. 2005).

We correlate the equivalent width of the H α line and parameters of the fitted Gaussian components with the light variations in Fig. 4. The top panel shows that there was an inverse correlation between the system’s apparent magnitude and the H α equivalent width. This indicates that the flare-up was largely a flare of continuum. The middle panel in Fig. 4 suggests, however, that line profile changes also accompany the flaring activity: of the three components, the blue and the broad ones narrowed significantly in the flare maximum. The formal error of the widths of the Gaussian fits is about 2-3%, which was definitely exceeded by the observed $\sim 11\%$ changes. It is very interesting that the width of the red component was very stable apart from a gradual broadening with time, indicating that it was formed in a completely different part of the system that did not take part in the flaring activity. Finally, the bottom panel in Fig. 4 shows the variations of the Doppler-shifts of the components with time. The individual errors are between 10–50 km s^{-1} , so the observed changes are real. Interestingly, they do not show any visible correlation with the flaring activity, suggesting the lack of strong asymmetries in line profile variations.

3.3 Paschen lines

In the near-infrared spectra we identify higher order lines of the Paschen series, all in emission, the He II $\lambda 8237$ line with a P Cygni

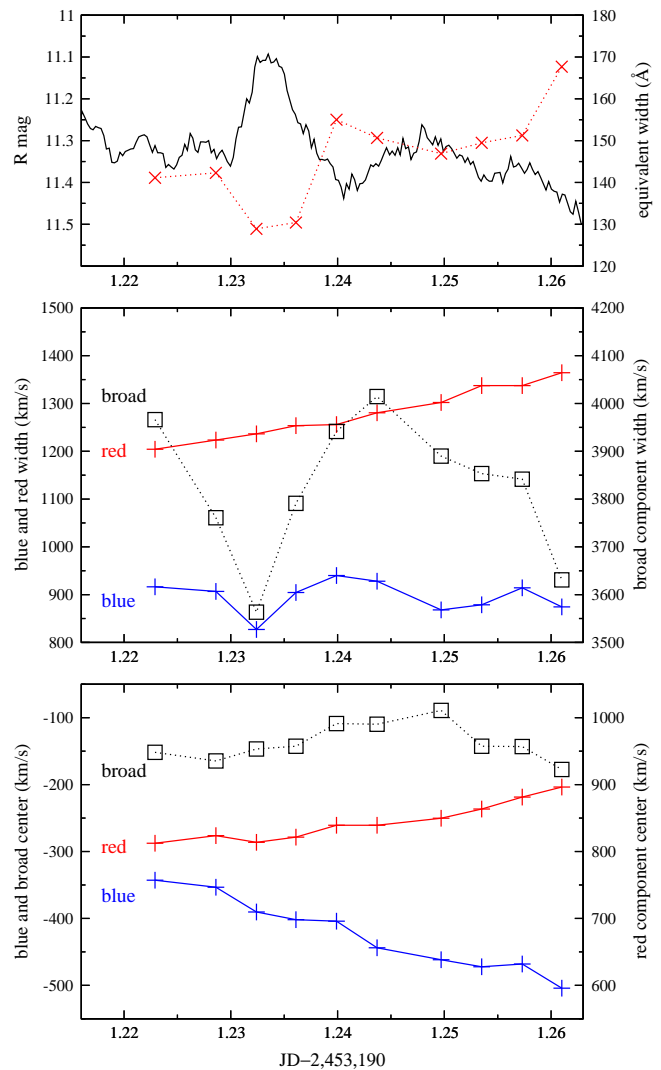


Figure 4. Line profile changes correlated with light variability. *Upper panel:* equivalent width of the H α line (red crosses with dotted line) and observed apparent magnitudes (solid line). The typical error of the equivalent width is a few Å. *Middle panel:* Time variations of the FWHMs of the three Gaussian components, expressed in km s^{-1} . Blue and red crosses show the blue and red components, while open squares refer to the broad component. *Bottom panel:* Time variations of the line centres of the Gaussian components. Symbols as in the middle panel.

profile and possibly some emission of the O I $\lambda 8446$ line. Due to the broadness of the features, there might be additional contamination from other species. For example, the P16, 15 and 13 lines could be contaminated by calcium emissions at 8498, 8542 and 8652 Å, respectively. We show a zoomed plot of the Paschen lines in Fig. 5, where the dashed-line spectrum was taken 5 hours later.

The Paschen lines changed significantly over the 5 hours between July 4.487 and 4.718 UT. These changes were similar both to those of the He I lines in the blue region and the He I $\lambda 6678$ line in the H α region, showing stronger red-shifted and blue-shifted emission components. The FWZI increased from 1000–1500 km s^{-1} up to 3000 km s^{-1} , which is also similar to that of the He I $\lambda 6678$ line. Finally, whereas the earlier spectrum showed comparable line strengths for the Paschen lines, this changed dramatically later, with the lower members of the series (P11 and P12) becoming much

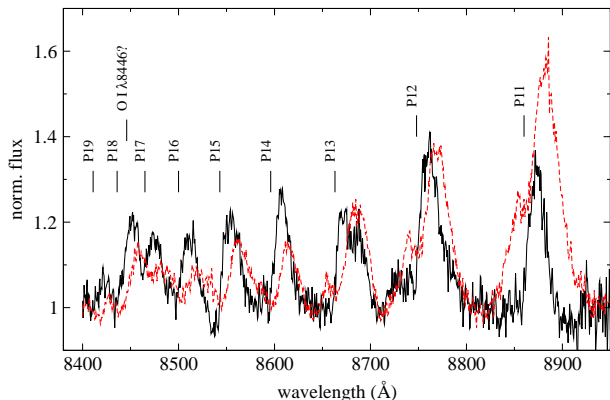


Figure 5. Lines of the Paschen series at July 4.487 UT (black/solid line) and July 4.718 UT (red/dashed line). Numbers indicate the order within the series.

stronger than the other lines. This is indicative of switching from optically thick to optically thin emission, where the latter is characterized by a regular flux increase toward the lower member of the series (see Storey & Hummer 1995 for theory and Clark et al. 1998 for an application in a Be/X-ray binary). We return to the implications of these spectra in Sect. 5.

4 RADIAL VELOCITIES IN QUIESCENCE

We continued regular observations of V4641 Sgr after it returned to quiescence. Our monitoring has resulted in further 46 spectra, taken between 2004 Sept. 25 and 2005 March 28. None of the spectra showed any sign of variability or spectral line distortion that might have occurred due to some accretion activity (Goranskij et al. 2003), with the only detectable change due to the orbital motion of the second component. Given that the one published radial velocity curve (Orosz et al. 2001) had quite large uncertainties (see fig. 2 in Orosz et al. 2001), we decided to re-determine spectroscopic elements of the system.

A sample quiescence spectrum is shown in Fig. 6. It is dominated by the strong $H\alpha$ absorption line, which is characteristic for a late B/early A type star. The strong Na I D doublet is of interstellar origin as its radial velocity does not change with the orbital phase. Apart from these, only weaker features of Mg II and Si II are easily identifiable, which agrees very well with the quiescence observations of Orosz et al. (2001). As a comparison, we also plot a spectrum of HR 3383, an A1V star. The close similarity of the spectra supports the spectral type determination by Orosz et al. (2001).

We decided to use the $H\alpha$ line for measuring radial velocities because: 1. the $H\alpha$ region was observed on every night, providing a homogeneous dataset; 2. this region is where the B9III-type secondary (Orosz et al. 2001) and the A/F-type radial velocity standards have the most similar spectra, minimizing the effects of spectral mismatch on cross-correlation (Verschueren et al. 1999); 3. all the other stellar features are almost lost in continuum scatter.

We determined heliocentric radial velocities using 200 Å of the spectra, centred on the $H\alpha$ line. As the primary standard we chose HD 187691, an F8V star, while β Vir (F9V) and HR 3383 (A1V) served as check stars for the absolute accuracy. We preferred the F-type standard over HR 3383 because of its narrower $H\alpha$ line, producing a slightly narrower cross-correlation peak. A period search of the radial velocities resulted in $P_{\text{spec}} = 2.817(2)$

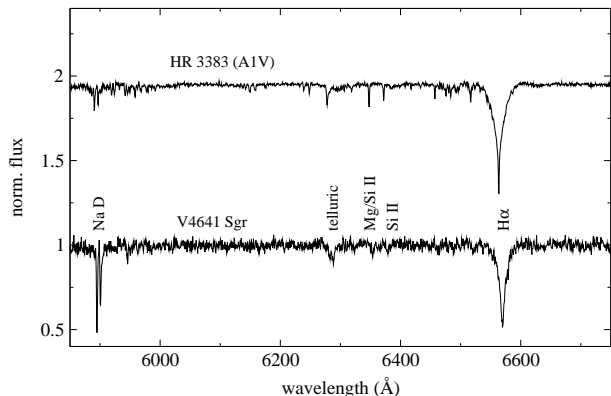


Figure 6. A sample DBS-red spectrum of HR 3383 (upper plot) and V4641 Sgr in quiescence (lower plot).

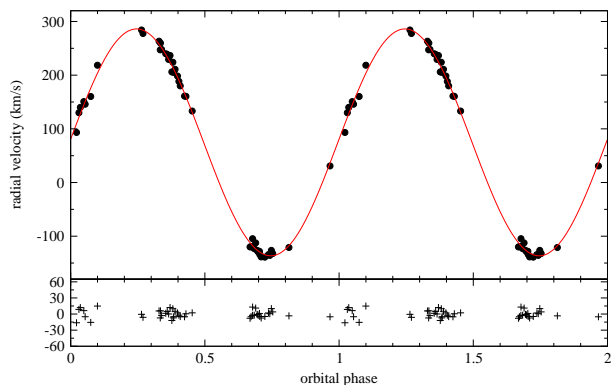


Figure 7. New radial velocity data phased according to the ephemeris in Eq. (1). The rms of the sine-wave fit is 7 km s^{-1} .

d, which is in good agreement with the period determined by Orosz et al. (2001), and is practically identical to the (more accurate) photometric period. For that reason, radial velocities were phased using the ephemeris in Eq. 1 and are plotted in Fig. 7. To estimate the measurement error, we took the residual mean scatter of the sine-wave fit (solid line in Fig. 7) and the scatter of the interstellar Na I D velocities, which were also determined with cross-correlation. Both estimates gave consistent results ($\sigma_{V_r} \approx 7 \text{ km s}^{-1}$) and the symbol sizes in Fig. 7 reflect this uncertainty.

To check whether Eq. 1 is consistent with the spectroscopic data, we also phased the data with the spectroscopic ephemeris obtained by Orosz et al. (2001): $P = 2.81678 \text{ d}$, $T_0 = 2451442.523$. The resulting phase diagram was shifted by $\Delta\phi = 0.10 \pm 0.01$ in respect to fig. 2 of Orosz et al. (2001), i.e. the minimum of the sine-wave occurred at $\phi = 0.60 \pm 0.01$. We used this shift to correct the Orosz et al. period to $P = 2.81720(2) \text{ d}$, indicating the good accuracy of the photometric period in Eq. 1.

The best fit sine-wave in Fig. 7 resulted in the following parameters: $K_2 = 211.3 \pm 1.0 \text{ km s}^{-1}$, $\gamma = 74.8 \pm 0.8 \text{ km s}^{-1}$. The K_2 velocity amplitude is in excellent agreement with that of Orosz et al. (2001), who measured $211.0 \pm 3.1 \text{ km s}^{-1}$. Combined with the period, the resulting mass-function is $f(M) = 2.74 \pm 0.04 M_{\odot}$. However, our γ -velocity differs by over 30 km s^{-1} (the Orosz et al. value is $\gamma = 107.4 \pm 2.9 \text{ km s}^{-1}$), i.e. over 10σ .

To determine the cause of the discrepancy, we first checked the consistency between different radial velocity standards. β Vir,

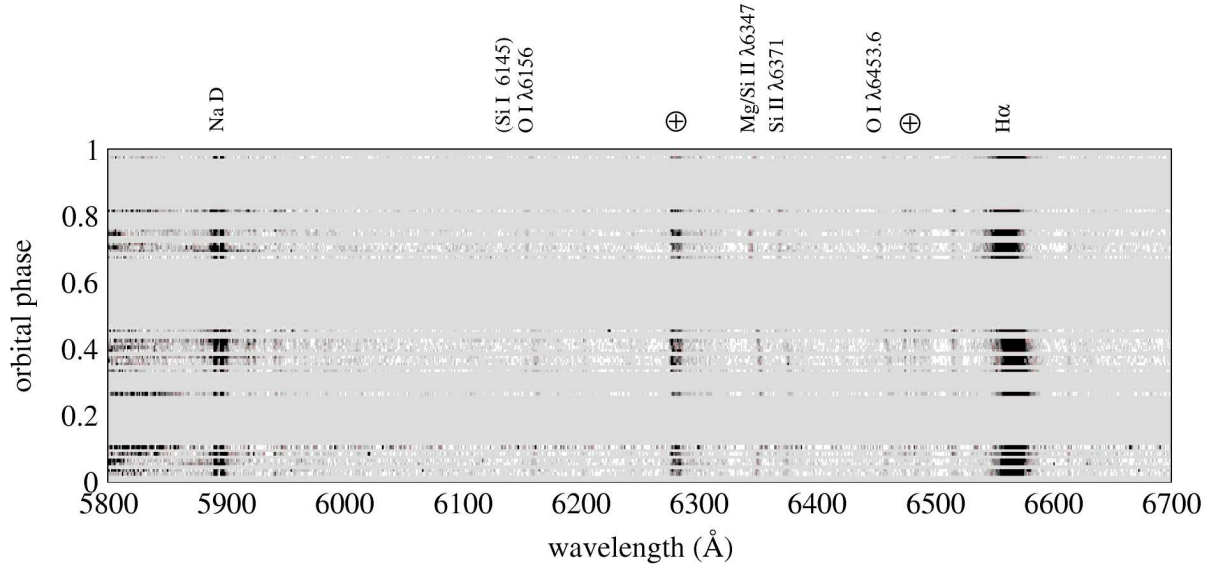


Figure 8. Trailed quiescence spectra of V4641 Sgr.

the other F-type standard, yielded essentially the same result, $\gamma = 75.2 \pm 0.8 \text{ km s}^{-1}$, while HR 3383, the A1V standard with broader H α line, gave $\gamma = 68.0 \pm 0.7 \text{ km s}^{-1}$ (the K_2 radial velocity amplitude was the same in all cases within the error bars). Note that the quoted errors came from the sine-wave fit, so that systematic errors are not included. From these numbers, it is obvious, that (i) the large difference between the HD 187691 velocities and those of Orosz et al. (2001) is real and (ii) despite the consistency of the two F-type standards, the HR 3383 velocities warn us that there might be larger systematic errors due to spectral mismatch than the raw data would suggest. In other words, it would be misleading to conclude from the two F-type standards that we have measured the γ -velocity within $\pm 0.6 \text{ km s}^{-1}$. On the other hand, the broader H α line of HR 3383 may enhance possible systematics in cross-correlation velocities (for instance, due to uncertainties in continuum normalization), so that the apparent offset between the F-type and A-type standards ($\sim 7 \text{ km s}^{-1}$) is likely to be more affected by the A-type HR 3383. Considering these aspects, we think the simple mean of the three values and its standard deviation give a more realistic γ -velocity and error estimate than, for instance, the average of the two F-type velocities. We adopted therefore $\gamma = 72.7 \pm 3.3 \text{ km s}^{-1}$ as our systemic velocity of V4641 Sgr.

We then noticed that in Sect. 2 of Orosz et al. (2001) its authors used a bright night sky emission line to match the wavelength scales of spectra taken in different observatories: “*The bright night sky emission line at $\approx 5578 \text{ \AA}$ was used to make small adjustments to the wavelength of the FLWO and VLT spectra. The shifts required to align this feature to a common wavelength (5578.0 \AA) were generally less than $\approx 15 \text{ km s}^{-1}$, although the VLT spectra from the end of the night of June 7 required shifts on the order of 80 km s^{-1} .*” We checked this line and found that it belongs to the neutral oxygen, for which the NIST Atomic Spectra Database² lists 5577.339 \AA as the laboratory wavelength. On the other hand, IRAF’s internal telluric line list (`linelists/skylines.dat`) contains two telluric features at 5577.3894 \AA and 5577.5948 \AA . These three wave-

lengths are $\sim 22 - 36 \text{ km s}^{-1}$ towards blue from the value used by Orosz et al. (2001), which suggests that the Orosz et al. data are offset by about 30 km s^{-1} . If we adopt the O I line from the NIST database, the Orosz et al. data should be corrected by 35.5 km s^{-1} , yielding a corrected γ -velocity of $71.9 \pm 2.9 \text{ km s}^{-1}$, which is in perfect agreement with ours. This is very reassuring, as the $\sim 30 \text{ km s}^{-1}$ shift in the centre-of-mass velocity over ~ 5 years could otherwise be explained only by a very massive invisible third body. This not only seems very unlikely, given the $14 - 20 M_{\odot}$ total mass of the binary (Orosz et al. 2001), but also lacks support from other observations.

Finally, we present the trailed quiescence spectra of V4641 Sgr in Fig. 8, in which we emphasize the weaker lines of the secondary star and the lack of spectral changes other than varying Doppler-shifts. Besides H α , five further lines (of O, Mg and Si) clearly showed the orbital motion. Other lines remained constant (except for a $\sim 30 \text{ km s}^{-1}$ scatter in the telluric lines due to the heliocentric corrections calculated with the `rvcor` and `dopcor` tasks). The stability of these spectra indicated a minimum level of mass-transfer activity during our observations.

5 DISCUSSION

5.1 Implications on outburst mechanisms

In black-hole X-ray binaries, emission lines are generally from an accretion disk. They have double-peak structures, typically with an equivalent width of $10\text{--}20 \text{ \AA}$ in H α (see a recent discussion in Wu et al. 2002). Additionally, their line profiles often have weak asymmetry due to orbital motion of a bright spot (e.g. Casares et al. 1995) or extended structures around the accretion disk (Soria et al. 2000).

The emission lines of V4641 Sgr are completely different from these typical results. Firstly, the lines are highly asymmetric, a feature which is difficult to attribute to the weak contribution of a bright spot. Secondly, the equivalent width of the H α is quite large, $130\text{--}170 \text{ \AA}$. The emitting area of lines should therefore have a volume at least five times that of the entire disk which argues against scenarios with local asymmetry in a disk. Furthermore, both Fe and

² http://physics.nist.gov/cgi-bin/AtData/lines_form

He lines show P Cygni profiles, which are not expected from an accretion disk. Consequently, instead of emission from a disk, the evidence points to a violent mass ejection and the presence of an outflow, which began optically thick in the Paschen lines and became optically thin within five hours. This suggests that the ejection was very limited in time and our observations covered the initial phase of shell expansion.

Although it has a very different character, we noticed a remarkable spectral similarity with the X-ray transient CI Cam (RXTE J0421+560). Robinson et al. (2002) presented $H\alpha$ and Paschen line profiles of the 1998 March/April outburst of CI Cam, which had the same broad blue extensions like V4641 Sgr in outburst. Hynes et al. (2002), whilst discussing their optical spectra which showed similar line profiles to ours, proposed a two-component outflow for CI Cam, with a fast, hot polar wind and a dense, cooler equatorial outflow with much lower velocity. However, the temperature of the secondary star in V4641 Sgr is too low to generate a strong stellar wind, so that the outflow is presumably from a disk, in other words, a disk wind.

Regarding this point, we found another noteworthy similarity, this time between V4641 Sgr and the famous galactic jet source, SS 433. Spectra taken from it show an $H\alpha$ emission line with both "moving" components, which are interpreted as optical jets, and a "stationary" component (for examples of the latter, see Murrin et al. (1980), Vermeulen et al. (1993) and Gies et al. (2002)). The profiles of this stationary line of SS 433 depend on its orbital phase. Consequently, it is very interesting that the emission line of V4641 Sgr, which was taken near an orbital phase of 0, is quite similar to the stationary component of SS 433 when its orbital phase = 0. Given that the stationary component in SS 433 is interpreted as originating from a disk wind, this provides further evidence for the same in V4641 Sgr. As both systems have a high inclination angle, the presence of a secondary star probably affects line profiles since it would block a part of the wind at an orbital phase = 0. This may cause a weaker blue component in $H\alpha$ and He lines of V4641 Sgr.

Inspired by the similarity with SS 433, we unsuccessfully tried to find possible "moving emission lines" for a sign of optical jets around the $H\alpha$ line of V4641 Sgr. A possible feature can be seen at about 6360 Å, but this is more likely to be due to atmospheric distortion of the Mg/Si II emissions. However, our spectral coverage was quite limited and we cannot firmly exclude the existence of "moving emission lines" outside the 6047–7005 Å region.

From a theoretical point of view, disk winds have been studied for cataclysmic variables, especially novalike systems. For example, Proga (2003b) calculated resonance-line profiles predicted by radiation-driven disk wind models for novalike systems. Some of his theoretical emission line profiles are similar to lines in V4641 Sgr and SS 433. However, despite the recent progress in the field (e.g. Feldmeier & Shlosman 1999, Feldmeier et al. 1999, Proga 2003a), the complexity of the problem prevents simple modeling of the observed line profiles. An important point is that this line-driven wind theory needs a strong UV radiation to accelerate the wind. The strong UV radiation can be expected from the surface of white dwarfs in cataclysmic variables. On the other hand, the UV radiation from black hole X-ray binaries is expected to be weaker, especially in a low/hard state of X-ray binaries. This is because a hot thermal accretion disk is truncated by an inner "radiation inefficient accretion flow" (RIAF).

The most fundamental difference between V4641 Sgr and SS 433 is their X-ray luminosities. The X-ray luminosity of SS 433 reaches super-Eddington luminosity for a $10 M_{\odot}$ black hole ($\sim 10^{39}$ ergs s^{-1}). According to theories of super-Eddington accre-

tion, the accreting gas forms an optically thick and geometrically thin disk (so called "slim disk", Abramowicz et al. 1988). This slim disk can generate strong UV radiation, which is favourable for the line-driven wind model. But, the X-ray luminosity of V4641 Sgr is about $\sim 10^{36-37}$ erg s^{-1} during minor outbursts. This value indicates a low/hard state, in which we cannot expect strong UV radiation.

In summary, the driving mechanism of the disk wind in V4641 Sgr remains an open issue. It is possible that the driving mechanism is not the UV radiation, but a magnetic field. Another possibility is that the accretion rate actually reached the super-Eddington level, but was undetected – perhaps because most of the X-ray radiation was absorbed by a thick torus around the black hole and reemitted in optical. Currently though, both scenarios are merely speculations.

Another important question is: to what extent was the 1999 "super-outburst" different from the smaller eruptions in 2002, 2003 and 2004? Based on the orders-of-magnitude lower X-ray emission in the later outbursts, Uemura et al. (2004a, 2005) concluded that all minor outbursts had the same nature, which was different from that of the 1999 September event. Uemura et al. (2004a) also proposed a scenario for the time evolution of the rapid brightness fluctuations: generation of a hot region in an accretion disk, which propagates towards the inner portion of the disk, triggering short-term fluctuations. When the active and bright region finally disappears, which is observed as a dip, the whole cycle repeats with the replenishment of gas from the outer region.

Our optical and near-infrared spectra suggest that despite the much weaker X-ray flux, mass ejection had very similar kinematic properties in 1999 September and 2004 July. Most noticeably, the description of the $H\alpha$ line in the 1999 outburst by Orosz et al. (2001) and Chaty et al. (2003) fits our observations in 2004 perfectly. The broad, strong emission lines and their variability (e.g. the He I $\lambda 5015$ and He I $\lambda 5049$ lines) suggest the presence of a high-velocity outflow component blown off from the accretion of matter on to the compact object. (Schulz & Brandt 2002, Chaty et al. 2003). The Paschen lines revealed the surprisingly short timescale of this blow-off. The first spectra contained strong emission in the upper lines, which is indicative of high density/optically thick lines (e.g. Lynch et al. 2000). Within five hours, upper Paschen lines strongly decreased, implying switching to optically thin emission, so that the blown-off matter did not have further supplies from the accretion disk. The variations of the $H\alpha$ equivalent width during a 10-min flare-up revealed that rapid brightness fluctuations are caused by continuum variations, therefore our observations are consistent with the Uemura et al. (2004a) scenario in a sense that the source of these continuum fluctuations must be in the inner part of the accretion disk.

We also found subtle changes in the $H\alpha$ line profile, which suggest the presence of additional phenomena during the rapid fluctuations: whereas the redshifted emission component did not show any correlation with the flare-up, the blue and the broad components exhibited significant changes in the velocity range of the emitting gas. Moreover, the gradual shifts with opposite signs in the line centre of the blue and red components support the contention that the three components (blue, red and broad) formed in well-separated parts of the system. The source of the red component must have been located far out on the accretion disk, as it was left unchanged by the flare. In contrast, the blue and broad components traced the continuum changes very well, suggesting they must have originated much closer to the disk, with the broad component being the closest.

5.2 System parameters

The outburst $H\alpha$ spectra allowed the detection of the 6613 Å Diffuse Interstellar Band (DIB) on the red wing of the $H\alpha$ profile. The equivalent width of this DIB is known to correlate with the interstellar reddening; adopting $EW_{6613}/E(B - V) \approx 0.231$ (Jenniskens & Désert 1994), the observed $EW_{6613} \approx 0.04 - 0.06$ Å yields $E(B - V) \approx 0.22 \pm 0.05$ mag. The sodium D doublet in quiescence is significantly stronger than reported for the 1999 outburst by Chaty et al. (2003): we measured the equivalent width of the sodium D_1 line between 0.8 Å–0.9 Å in the best quiescence spectra, which is about twice as much as the 0.45 Å observed by Chaty et al. (2003). However, our spectra have reasonably better resolving power ($R \sim 6000$ vs. ~ 270) and the given EW_{D_1} suggests slightly higher reddening, between 0.4–0.6 mag (see fig. 4 in Munari & Zwitter 1997). Considering the large uncertainties, these reddenings are consistent with the previous determinations: $E(B - V) = 0.32 \pm 0.10$ mag (Orosz et al. 2001) and $E(B - V) \approx 0.25$ mag (Chaty et al. 2003).

Our radial velocity curve has the smallest uncertainties in the literature so far; the K_2 velocity amplitude (211.3 ± 1.0 km s⁻¹) and the corresponding mass-function (2.74 ± 0.04 M_⊙) are the same as those of by Orosz et al. (2001). The most significant improvement is found for the centre-of-mass velocity of the system, for which we adopt the mean value of the three independent measurements: $\gamma = 72.7 \pm 3.3$ km s⁻¹. Assuming that this systemic velocity is due entirely to differential galactic rotation, we slightly revise the kinematical distance limit to $d > 6.3$ kpc, using the rotation curve given in Fich et al. (1989) and the standard IAU rotation constants of $R_0 = 8.5$ kpc and $\Theta_0 = 220$ km s⁻¹ (from $d > 7$ kpc, Orosz et al. 2001). When combined with accurate distance and proper motion measurements, the γ -velocity will be important in finding the galactocentric orbit of V4641 Sgr. Knowing the galactic motion of an X-ray binary can help understand the possible origin of the system, which in turn can reveal intriguing details of star formation in the early stages of evolution of the Galaxy (Mirabel et al. 2001, 2002, Mirabel & Rodrigues 2003).

6 SUMMARY

We have presented optical and near-infrared spectra of the galactic microquasar V4641 Sgr in a short outburst in 2004 July and quiescence between 2004 September–2005 March. The conclusions can be summarized as follows:

(i) The photometric behaviour of the 2004 July outburst was similar to those in 2002 and 2003, i.e. the star showed rapid brightness fluctuations, due to changes in the continuum radiation. However, the complex multi-component emission line profiles of hydrogen, helium and iron were similar to those observed in the big outburst of 1999 September, with evidence of a similar high-velocity outflow and optically thick and then thin emission. This suggests that kinematic properties of the mass-ejection processes were similar in 1999 and 2004 despite the huge difference in peak luminosities of the eruptions.

(ii) We have determined the most accurate radial velocity curve of the system so far. We confirm the optical mass function of the system by Orosz et al. (2001) reducing its uncertainty by a factor of three to $f(M) = 2.74 \pm 0.04$ M_⊙. We correct the systemic velocity by more than 30 km s⁻¹ to $\gamma = 72.7 \pm 3.3$ km s⁻¹. We do not find spectral changes other than the Doppler-shifts due to

the orbital motion, so any accretion activity must have been at low levels during our quiescence observations.

(iii) In the last couple of years it has been clearly established that V4641 Sgr has a recurrent activity with a time-scale of 1–2 years. Looking back, the shorter value seems to be more appropriate, which means every observing season should be monitored for further eruptions. Our findings demonstrate the importance of taking rapid spectroscopic snapshots right after the discovery of a new outburst. We suggest to keep the object on lists of possible target-of-opportunity observations, because collecting more information on spectral changes in early phases is expected to yield better understanding of interactions around the black holes in systems like V4641 Sgr, especially the nature of mass ejection and its connection to the accretion disk.

ACKNOWLEDGMENTS

This work has been supported by the OTKA Grant #T042509 and the Australian Research Council. C. Lindstrøm received a Vacation Scholarship for this project from the School of Physics, University of Sydney. L.L. Kiss is supported by a University of Sydney Postdoctoral Research Fellowship. A. Derekas joined the project within the International Postgraduate Research Scholarship scheme of the Australian Department of Education, Science and Training. The authors thank Prof. R.W. Hunstead for a careful reading of the manuscript. The NASA ADS Abstract Service was used to access data and references.

REFERENCES

- Abramowicz M. A., Czerny B., Lasota J. P., & Szuszkiewicz E., 1988, *ApJ*, 332, 646
- Bikmaev I., Khamitov I., Aslan Z., Sakhbullin N., Burenin R., Pavlinsky M., Revnivtsev M., & Sunyaev R., 2004, *The Astronomer's Telegram* No. 309
- Buxton M., Bailyn C., & Maitra D., 2005, *The Astronomer's Telegram* No. 542
- Casares J., et al., 1995, *MNRAS*, 274, 565
- Chaty S., Charles P. A., Martí J., Mirabel I. F., Rodríguez L. F., & Shahbaz T., 2003, *MNRAS*, 343, 169
- Clark J. S., Steele I. A., Coe M. J., & Roche P., 1998, *MNRAS*, 297, 657
- Feldmeier A., & Shlosman I., 1999, *ApJ*, 526, 344
- Feldmeier A., Shlosman I., & Vitello P., 1999, *ApJ*, 526, 357
- Fich M., Blitz L., Stark A. A., 1989, *ApJ*, 342, 227
- Gies D. R., McSwain M. V., Riddle R. L., Wang Z., Wiita P. J., & Wingert D. W., 2002, *ApJ*, 566, 1069
- Goranskij V. P., Barsukova E. A., & Burenkov A. N., 2003, *Astron. Reports*, 47, 740
- Hjellming R. M., et al., 2000, *ApJ*, 544, 977
- Hynes R. I., et al., 2002, *A&A*, 392, 991
- in't Zand J., Heise J., Bazzano C., Cocchi M., Di Ciolo L., Muller J. M., 1999, *IAU Circ.* 7119
- Jenniskens P., & Désert F.-X., 1994, *A&AS*, 106, 39
- Khamitov I., et al., 2005, *The Astronomer's Telegram*, No. 540
- Kiss L. L., & Mészáros Sz., 2004, *The Astronomer's Telegram*, No. 299
- Lynch D. K., Rudy R. J., Mazuk S., & Puetter R. C., 2000, *ApJ*, 541, 791
- Markwardt C., Swank J., & Marshall F., 1999, *IAU Circ.* 7120
- Mirabel I. F., & Rodrigues I., 2003, *A&A*, 398, L25
- Mirabel I. F., Dhawan V., Mignani R. P., Rodrigues I. & Guglielmetti F., 2001, *Nature*, 413, 139
- Mirabel I. F., Mignani R., Rodrigues I., Combi J. A., Rodríguez L. F., & Guglielmetti F., 2002, *A&A*, 395, 595
- Munari U., & Zwitter T., 1997, *A&A*, 318, 269

- Murdin P., Clark D. H., & Martin P. G., 1980, MNRAS, 193, 135
- Orosz J. A. et al., 2001, ApJ, 555, 489
- Proga D., 2003a, ApJ, 585, 406
- Proga D., 2003b, ApJ, 592, L9
- Revnivtsev M., Khamitov I., Burenin R., Pavlinsky M., Sunyaev R., Aslan Z., Bikmaev I., & Sakhbullin N., 2004, The Astronomer's Telegram, No. 297
- Robinson E. L., Ivans I. I., & Welsh W. F., 2002, ApJ, 565, 1169
- Rupen M. P., Mioduszewski A. J., Dhawan V., 2004, The Astronomer's Telegram, No. 296
- Schulz N. S., & Brandt W. N., 2002, ApJ, 572, 971
- Soria R., Wu K., & Hunstead R. W., 2000, ApJ, 539, 445
- Storey P. J., & Hummer D. G., 1995, MNRAS, 272, 41
- Stubbings R., 1999, IAU Circ. 7253
- Swank J., 2004, The Astronomer's Telegram, No. 295
- Swank J.H., Smith E. A., & Markwardt C. B., 2005, The Astronomer's Telegram, No. 536
- Uemura M., et al., 2002, PASJ, 54, L79
- Uemura M., et al., 2004a, PASJ, 56, 823
- Uemura M., et al., 2004b, PASJ, 56, S61
- Uemura M., et al., 2005, IBVS, No. 5626
- Vermeulen R. C., et al., 1993, A&A, 270, 204
- Verschueren W., David M., & Griffin R. E. M., 1999, A&AS, 140, 107
- Wijnands R., & van der Klis M., 2000, ApJ, 528, L93
- Wu K., Soria R., Johnston H., Hunstead R., 2002, in: Proc. of The Ninth Marcel Grossmann Meeting, Eds.: Vahe G. Gurzadyan, Robert T. Jantzen, Remo Ruffini, World Scientific Publishing, p. 2274 (full text as astro-ph/0101390)